Geophysical Research Letters

RESEARCH LETTER
10.1029/2019GL082360

Key Points:
- GEOS-Chem accurately modeled the initial transport of pyrocumulonimbus aerosols showing a similar 5-month lifetime as volcanic aerosols
- Positive radiative forcing of pyroCb aerosols (+) can be similar in magnitude but opposite in sign of forcings from volcanic aerosols (−)
- Direct injection of smoke aerosols into the modeled stratosphere was required for modeled and satellite-measured aerosol profiles to agree

Supporting Information:
- Supporting Information S1

Correspondence to:
J. Wang and K. Christian,
jun-wang-1@uiowa.edu;
kenneth.e.christian@nasa.gov

Citation:
Christian, K., Wang, J., Ge, C., Peterson, D., Hyer, E., Yorks, J., & McGill, M. (2019). Radiative forcing and stratospheric warming of pyrocumulonimbus smoke aerosols: First modeling results with multisensor (EPIC, CALIPSO, and CATS) views from space. *Geophysical Research Letters*, *46*, 10,061–10,071. https://doi.org/10.1029/2019GL082360

Received 17 FEB 2019
Accepted 23 JUL 2019
Accepted article online 29 JUL 2019
Published online 20 AUG 2019

Radiative Forcing and Stratospheric Warming of Pyrocumulonimbus Smoke Aerosols: First Modeling Results With Multisensor (EPIC, CALIPSO, and CATS) Views from Space

Kenneth Christian[1,2,3], Jun Wang[1,2], Cui Ge[1,2], David Peterson[4], Edward Hyer[4], John Yorks[5], and Matthew McGill[5]

[1]Department of Chemical and Biochemical Engineering, The University of Iowa, Iowa City, IA, USA, [2]Center for Global and Regional Environmental Research, The University of Iowa, Iowa City, IA, USA, [3]Now at NASA Postdoctoral Program, NASA Goddard Space Flight Center, Greenbelt, MD, USA, [4]Naval Research Laboratory, Monterey, CA, USA, [5] NASA Goddard Space Flight Center, Greenbelt, MD, USA

Abstract Smoke particles can be injected by pyrocumulonimbus (pyroCb) in the upper troposphere and lower stratosphere, but their effects on the radiative budget of the planet remain elusive. Here, by focusing on the record-setting Pacific Northwest pyroCb event of August 2017, we show with satellite-based estimates of pyroCb emissions and injection heights in a chemical transport model (GEOS-Chem) that pyroCb smoke particles can result in radiative forcing of ~0.02 W/m^2 at the top of the atmosphere averaged globally in the 2 months following the event and up to 0.9 K/day heating in the Arctic upper troposphere and lower stratosphere. The modeled aerosol distributions agree with observations from satellites (Earth Polychromatic Imaging Camera [EPIC], Cloud-Aerosol Transport System [CATS], and Cloud-Aerosol Lidar with Orthogonal Polarization [CALIOP]), showing the hemispheric transport of pyroCb smoke aerosols with a lifetime of 5 months. Hence, warming by pyroCb aerosols can have similar temporal duration but opposite sign to the well-documented cooling of volcanic aerosols and be significant for climate prediction.

Plain Language Summary Extreme fire events can produce towering smoke plumes, which can result in the injection of smoke aerosols into the lower stratosphere (~10 km above the surface in the midlatitudes). These stratospheric aerosols are significant because they stay in the atmosphere longer than those closer to the surface. In this study, we modeled the effects emanating from one of the largest of these fire events that happened in British Columbia, Canada, and Washington, USA, on 12 August 2017. We found that the smoke particles from this fire event had a lifetime of around 5 months and resulted in a net positive radiative forcing with warming focused in the stratosphere because smoke particle contain soot, an efficient absorber of solar radiation. This net positive radiative forcing contrasts with the cooling effects of analogous volcanic eruptions that are long thought to be dominant sources of stratospheric aerosols. Accounting for these smoke aerosols from large forest fire events in studies of atmospheric composition and climate may be more significant in the future as more large fire events are expected in a warmer climate.

1. Introduction

Forest fires are well-documented ecological disruptors and can have a large impact on both local and regional air quality. The largest of these fire events can trigger cumulus clouds called pyrocumulus (pyroCu) lofting fire emissions well into the free troposphere (Fromm et al., 2005; Peterson et al., 2016). In the more extreme cases, this convection can lead to fire-generated thunderstorms, called pyrocumulonimbus (pyroCb). This intense convection can result in clouds overshooting the tropopause, lofting smoke aerosols many kilometers into the stratosphere (e.g., Fromm et al., 2000, 2005; Peterson et al., 2014). These higher altitudes are significant for smoke injections because aerosols in the upper troposphere and lower stratosphere (UTLS) have much longer residence times (months to years) compared to those in the lower troposphere and boundary layer (on the order of days) and are subject to longer-range transport (Barnes & Hofmann, 1997;

Ge et al., 2016; Koch et al., 2009; Robock, 2000; Wang et al., 2013). While infrequent, dozens of pyroCb plumes occur in the middle to high latitudes on a yearly basis representing an uncertain source of carbonaceous aerosols (Peterson et al., 2016).

Aerosols in the UTLS have effects on both the radiative balance of the planet and atmospheric chemistry. While we have long known the vast majority of aerosols in these reaches of the global atmosphere are sulfate (Turco et al., 1982), small but nonnegligible concentrations of carbonaceous aerosols have been noted as well going back into the 1980s (Clarke et al., 1983; Woods & Chuan, 1983) with black carbon (BC) representing around 1% of UTLS aerosol mass (Schwarz et al., 2008). Even at small concentrations, BC aerosols are significant as they are highly absorptive of solar and near-infrared radiation (Kremser et al., 2016; Ramanathan & Carmichael, 2008). In fact, anthropogenic BC emissions in the troposphere may have a climate forcing similar to that of methane (Andreae et al., 2004; Myhre et al., 2013). These warming effects can be augmented if the BC aerosols are internally mixed with sulfates, increasing their surface area and warming potential (Jacobson, 2001). Also, these carbon aerosols affect ice nucleation and cloud formation in the UTLS, which is highly uncertain in climate modeling (Bond et al., 2013). While pyroCbs have been noted to commonly inject aerosols well into the UTLS (e.g., Fromm et al., 2005), their effects on the UTLS aerosol concentrations and radiative balance of the planet remain uncertain.

An opportunity to explore the effects of pyroCb events on the global climate system arose on 12 August 2017 when fires in Washington (USA) and British Columbia (Canada) caused one of the largest pyroCb events in the observational record. This pyroCb event (hereafter the Pacific Northwest event) initiated as an advancing cold front from the Pacific Ocean provided the necessary meteorology for pyroCb convection. Cold fronts are common prerequisites for pyroCb initiation as the prefrontal environment typically features a hot and dry mixed layer that supports fire growth surmounted by a mid-level moisture source that supports deep, moist convection (Fromm et al., 2010; Peterson et al., 2014, 2018). By the end of 12 August, five individual fires had initiated pyroCb plumes from northern Washington through central British Columbia. This event injected between 0.1 and 0.3 Tg of smoke particle mass into the stratosphere, which is the largest known stratospheric intrusion from pyroCb activity, roughly comparable to the magnitude of a moderate volcanic eruption (Peterson et al., 2018) and resulted in a stratospheric plume of aerosols that encircled the Northern Hemisphere within a few weeks (Khaykin et al., 2018; Peterson et al., 2018). After the pyroCb event, Khaykin et al. (2018) showed from both ground-based lidar in France and satellite-based lidar there was a persistent layer of stratospheric aerosols attributable to the pyroCb event in altitudes exceeding 20 km. While Peterson et al. (2018) and Khaykin et al. (2018) both argued that the pyroCb event had a hemisphere-scale impact on stratospheric aerosol loading similar in magnitude to moderate volcanic events, no estimates of radiative forcings or simulation of transport were conducted.

To quantify the effects of pyroCb events on the global carbonaceous aerosol budget and the radiative balance of the planet, we represent the Pacific Northwest event in a global chemical transport model (CTM). Using a combination of pyroCb emission estimates from Peterson et al. (2018), the GEOS-Chem CTM, satellite lidar observations, and a radiative transfer model, we demonstrate the capacity of global CTMs, with constraints from satellite observations, to represent pyroCb events allowing for the quantification of their impacts on atmospheric composition and their radiative forcing.

2. Data and Models

2.1. CTM and Radiative Transfer Calculations

The CTM used for this study is GEOS-Chem (v11). GEOS-Chem has been a valuable tool in understanding global air chemistry since its introduction into the literature (Bey et al., 2001) and is widely used for a variety of air chemical applications. Aerosols are simulated in the model through a scheme derived from the Georgia Tech/Goddard Global Ozone Chemistry Aerosol Radiation and Transport model (Chin et al., 2002) with updates to the carbonaceous aerosol, ammonia, and secondary organic aerosol treatment by Park et al. (2003). Modeled BC and organic carbon (OC) are partitioned into hydrophobic and hydrophilic categories. Except as later noted with biomass burning emissions, we use the default model settings at $2° \times 2.5°$ horizontal resolution. The model is driven by archived GEOS-5 Forward Processing meteorology that is generated from the GEOS data assimilation system (Lucchesi, 2017).

Biomass burning emissions for the GEOS-Chem CTM generally come from either the Global Fire Emissions Database (GFED) (van der Werf et al., 2010) or Fire INventory from National Center for Atmospheric

Research (FINN) emission inventories (Wiedinmyer et al., 2011). While these inventories are sufficient for many studies, they are not sufficient for studies of specific fire events, like pyroCbs, because they do not have the necessary temporal resolution to resolve individual fires, do not contain any information about the three-dimensional nature of the smoke plume, and do not include direct stratospheric injection of smoke aerosols. Thus, in order to replicate pyroCb events in GEOS-Chem, we created a supplementary 3-D smoke aerosol inventory of the Pacific Northwest event for input into the model (see section 3.1)

To compute the radiative forcing from this pyroCb event, we use the Fu-Liou model, a delta-four-stream radiative transfer model (Fu & Liou, 1993, 1992). This particular model is used both off-line and online with various global, regional, and climate models (Gu et al., 2006; Ge et al., 2016; Wang et al., 2008). Shortwave radiative forcing and heating rate calculations are completed every 6 hr for six shortwave bins between 0.2 and 4 μm for each aerosol type, such as BC and OC, individually before the net forcing from the smoke aerosols is found. Optical properties, such as albedos, extinction coefficients, and asymmetry coefficients, vary by relative humidity for the hydrophilic BC and OC species and are described in Kopacz et al. (2011) and Wang et al. (2006).

2.2. Satellite Data

Satellite-based lidar such as CATS (Cloud-Aerosol Transport System) and CALIOP (Cloud-Aerosol Lidar with Orthogonal Polarization) are unmatched in providing high-resolution cloud and aerosol profiles. Measurements from CALIOP, aboard the Cloud-Aerosol Lidar Infrared Pathfinder Satellite Observations (CALIPSO) spacecraft (Winker et al., 2009), have been available since its launch into the A-Train constellation of Earth observing satellites in April of 2006 and CATS (McGill et al., 2015; Yorks et al., 2016) since its placement on the International Space Station in January of 2015. Because the sensors fly in different orbits, CATS observations are not available for high-latitude regions, such as some of the northern domains in this study.

Satellite-based lidar instruments can provide high-resolution information about the vertical distribution of aerosols along the lidar path, but they cannot provide information about the horizonal spatial distribution of the plume. For model comparison, we also employ the Earth Polychromatic Imaging Camera (EPIC) ultraviolet aerosol index (UVAI) on the Deep Space Climate Observatory satellite (Marshak et al., 2018; Xu et al., 2017). The Deep Space Climate Observatory satellite has provided measurements of the sunlit side of the Earth every 1 to 2 hr from its Lagrange-1 vantage point since 2015. As a qualitative measure of both the abundance and altitude of atmospheric aerosols, UVAI products have been available from various satellite instruments since TOMS in 1979 (Herman et al., 1997; Torres et al., 1998). UVAI can be calculated even in the presence of clouds, which is a valuable advantage over other satellite aerosol measures because plumes eminating from pyroCb events can be spatially colocated with clouds. In contrast, cloud contamination is not a serious consideration for the satellite lidar observations in this study since the pyroCb plume was located above tropospheric clouds.

3. Methods

In the following section we describe the steps taken to simulate the pyroCb event and its propagation in GEOS-Chem: creating the pyroCb emission event inventory, integrating these into GEOS-Chem, and designing numerical experiments for model evaluation and forcing calculations.

3.1. Creation of 3-D PyroCb Emissions

To represent the vertical variation in the smoke plumes and to allow for direct stratospheric injection of pyroCb smoke emissions, we must incorporate injection heights with the pyroCb emission estimates from Peterson et al. (2018). Altitude of emission injection has been shown in many previous studies to be significant in determining aerosol transport and residence time (Colarco et al., 2004; Field et al., 2016; Leung et al., 2007; Turquety et al., 2007; Val Martin et al., 2010). Similarly, modeled radiative forcings can also be sensitive to emission injection heights (Ban-Weiss et al., 2012; Wang & Christopher, 2006). Studies modeling volcanic events found modeled radiative forcings to be highly sensitive to emission injection heights due to the longer residence times of higher-altitude aerosols (Ge et al., 2016; Wang et al., 2013). For biomass burning, these injection heights can range from typical boundary layer height to the free troposphere and higher for large, intense fires such as those responsible for pyroCbs (Paugam et al., 2016). Previous attempts in integrating injection heights to emission inventories are split as to choices in the vertical distribution of the emissions with some emitting equally in model layers and others choosing their own assumptions as to

the vertical distribution (e.g., Leung et al., 2007). Since smoke plumes mix during transport over the long distances, the resultant smoke plume is not especially sensitive to the vertical distribution of the emissions, provided the injection height is the same (Wang et al., 2006). Thus, the regular injection height treatment of splitting emissions evenly from the injection height to the surface is sufficient for this application with some minor changes. As the emission estimates from Peterson et al. (2018) represent the total stratospheric injection, we emit 0.2 Tg of the 0.1 to 0.3 Tg estimated pyroCb plume at the specified injection height (13.7 km) with another 0.2 Tg split equally among the remaining vertical model layers from the injection height to the surface to track the propagation of the tropospheric smoke emissions. The pyroCb emission fluxes ($kg \cdot m^{-2} \cdot s^{-1}$) for each model layer are determined through equation (1) (F_l) and for the specified injection height in equation (2) (F_z).

$$F_{(l<z)} = \frac{(0.5 * M_{\mathrm{PCB}})}{(N_{\mathrm{hours}} * A_{1x1} * z)} \tag{1}$$

$$F_z = \frac{(0.5 * M_{\mathrm{PCB}})}{(N_{\mathrm{hours}} * A_{1x1})}. \tag{2}$$

Here l represents any model layer from the closest to the surface to the layer z corresponding to the injection height, M_{PCB} is the total mass of the pyroCb emission, in our case 0.4 Tg (0.2 Tg for the highest layer and 0.2 Tg for the lower layers), N_{hours} is the length of the pyroCb event (5 hr in our case from 19:00–23:59 UTC), and A_{1x1} is the 1° x 1° grid box area (m^2). Emission rates are determined as the emission fluxes are read into GEOS-Chem and depend on the thickness of the model layers.

To integrate the 3-D pyroCb emission fluxes into GEOS-Chem, we created an extension for the Harvard-National Aeronautics and Space Administration Emissions Component (Keller et al., 2014). Harvard-National Aeronautics and Space Administration Emissions Component is the tool by which emissions are calculated and coupled with GEOS-Chem. In our extension, the pyroCb smoke fluxes are read and partitioned via emission factors typical of extratropical forests into both BC (6%) and OC (94%; van der Werf et al., 2010). We only considered pyroCb smoke aerosol emissions in this study, but future work may expand the extensions scope to include trace gas emissions as well.

3.2. Experiment Design

To determine the impacts of the Pacific Northwest pyroCb event on the global atmosphere, we present both the model results from a stratospheric injection of smoke aerosols and a sensitivity test emitting the same mass into the near surface layer from the event on 12 August 2017 to the end of December 2017. This boundary layer sensitivity test is designed to demonstrate the necessity of direct UTLS emission of these aerosols as emitting biomass burning emissions into the near surface layer is the default mode in GEOS-Chem and other models. In our modeled results, we present the differences between a control case without the pyroCb emissions and two model runs: one featuring stratospheric injection of the pyroCb emissions and one featuring an injection of the pyroCb emissions into the boundary layer. Showing the differences between these two different emission injection scenarios and a control case allows us to isolate the effects of the pyroCb event. Radiative forcings were determined from the differences between the outgoing shortwave fluxes at the top of the atmosphere in the control case and the stratospheric injection case. For comparison to EPIC UVAI measurements we matched the modeled smoke (BC + OC) optical depth (550 nm) and for the vertical model evaluation we compared the modeled layer aerosol extinction (aerosol optical depth [AOD] divided by the vertical layer height) to CALIOP and CATS backscatter.

4. Results

4.1. Transport and Evolution of the Pyrocb Plume

A week after the pyroCb event, the resultant smoke plume had passed over the Canadian Arctic and had become enveloped in a frontal system over the North Atlantic as observed by EPIC. Over this time period, the smoke plume split into two features: the primary plume wrapped around the midlatitude cyclone over the North Atlantic and a secondary plume stretching from northern Greenland to the Canadian Arctic Archipelago (Figure 1a). With stratospheric injection of the pyroCb emissions, GEOS-Chem replicates these features (Figure 1b). When the emissions from the pyroCb event are emitted into the boundary layer in GEOS-Chem (Figure 1c), we find similar 2-D distributions but considerably lower smoke AODs. Specifically, the peak AOD in the main stratospheric plume is around 0.8 where the boundary layer test results in a

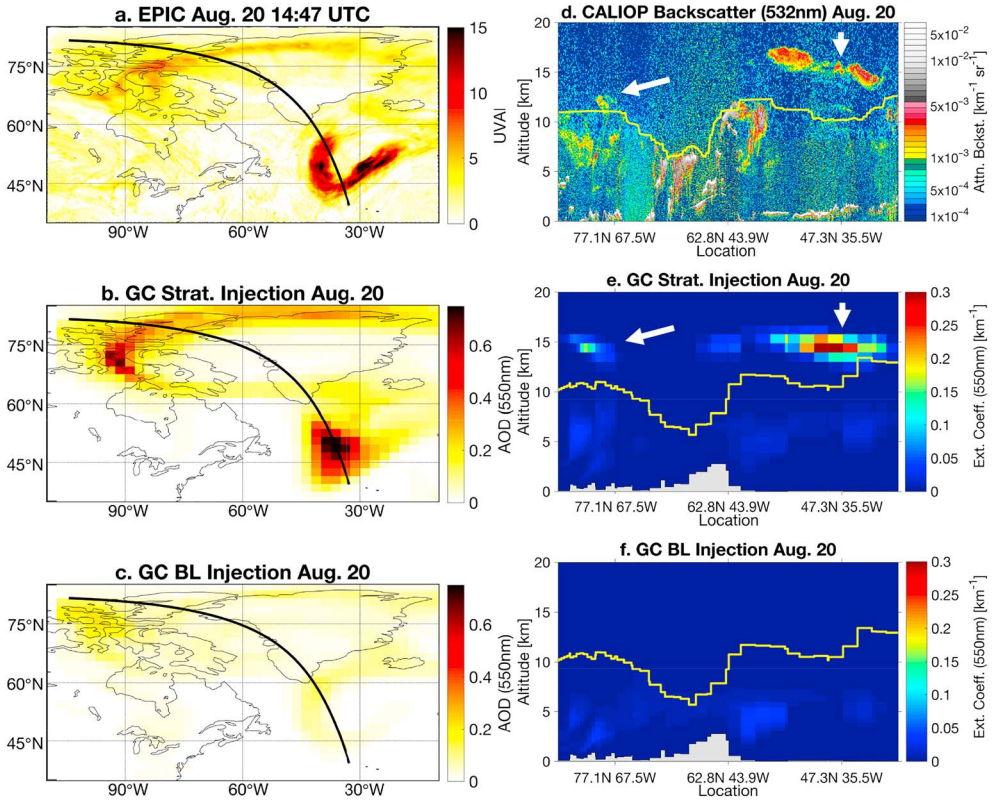

Figure 1. Agreement between satellite observations (EPIC ultraviolet aerosol index [a] and CALIOP total attenuated backscatter [d]) and GC modeled pyroCb smoke with stratospheric (AOD [b] and extinction coefficient [e]), and boundary layer (AOD [c] and extinction coefficient [f]) injections on 20 August 2017 about a week after pyroCb event. Black lines in (b) and (c) denote CALIOP orbit, and yellow lines in (d)–(f) represent tropopause altitude. White arrows point to locations of both the primary plume over the North Atlantic (right), and secondary plume over the Arctic (left). AOD = aerosol optical depth; CALIOP = Cloud-Aerosol Lidar with Orthogonal Polarization; EPIC = Earth Polychromatic Imaging Camera; GC = GEOS-Chem.

peak around 0.1 for the same location over the North Atlantic. This is due to higher-altitude aerosols having longer lifetimes than those closer to the surface. In addition, we find the model results with stratospheric injection of pyroCb smoke aerosols to qualitatively match EPIC UVAI observations on both August 14 and 19 (Figures S1 and S2). However, we note that the modeled plume location on August 14 is displaced to the west of the observed plume perhaps from errors in transport.

Vertically, GEOS-Chem captures both the main plume located over the North Atlantic and the secondary plume over the high Arctic as observed by the CALIOP overpass on 20 August (Figures 1d and 1e). The primary plume over the North Atlantic is clearly represented in the modeled results (Figure 1e), albeit 2–3 km lower in altitude than that observed by the CALIOP overpass. The secondary plume in the north is also captured in the model but ~2-km higher altitude than that observed by CALIOP. Part of the reason for the lower altitude of the modeled primary plume could be the lack of "self-lifting" or diabatic heating of smoke aerosols in the model (Wang & Christopher, 2006). Self-lifting has been noted in previous pyroCb cases to result in the continued vertical ascent of carbonaceous plumes in the stratosphere (de Laat et al., 2012; Siddaway & Petelina, 2011). In contrast, where the boundary layer injection in GEOS-Chem resulted in a similar aerosol distribution to those observed, Figure 1f shows that GEOS-Chem fails to capture the observed CALIOP vertical profiles with boundary layer injections. Specifically, no smoke aerosols were modeled in the altitudes CALIOP observed the smoke plume. Similar results were found with a CALIOP overpass on 14 August (Figure S1 in the supporting information) and a CATS overpass on 19 August (Figure S2). Hughes et al. (2016) similarly showed that if the injection height used to initiate the GEOS model is not correctly placed in the UTLS, predicted volcanic plume transport patterns do not agree with satellite observations. These results show that modeling pyroCb events and other large forest fire events in CTMs similarly require high-altitude injections of biomass burning emissions.

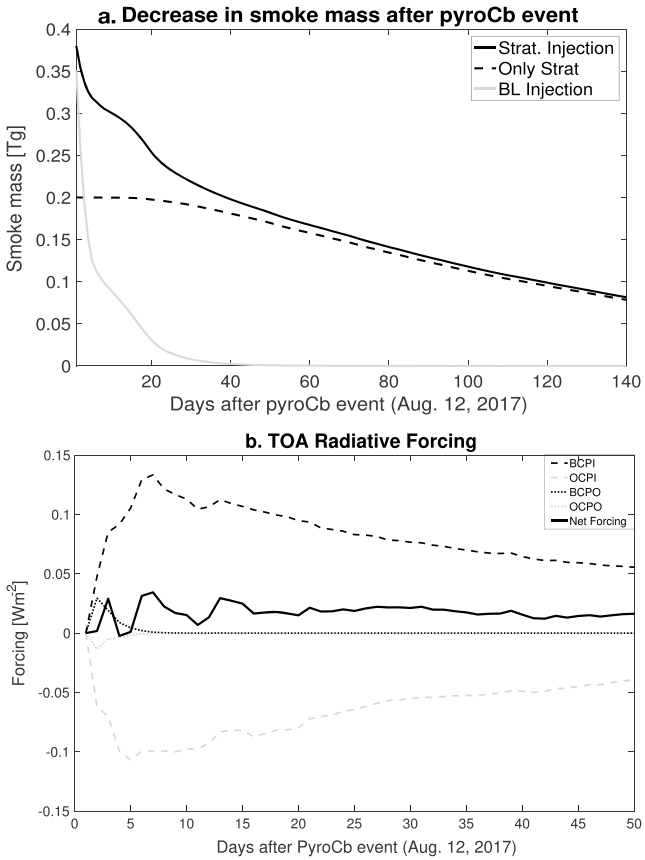

Figure 2. Decrease in modeled pyroCb smoke mass (a) and modeled radiative forcing after pyroCb event. Black and gray lines in (a) show differences between stratospheric injection (black) and boundary layer (gray) emission injection with the black dashed line showing the decrease in the 0.2 Tg emitted into the stratosphere. Solid black line in (b) shows net radiative forcing at the top of the atmosphere (TOA), and dashed and dotted lines show TOA radiative forcings from hydrophilic (dashed) and hydrophobic (dotted) black carbon (black) and organic carbon (gray; e.g., BCPI = hydrophilic black carbon, BCPO = hydrophobic black carbon, OCPI = hydrophilic organic carbon, OCPO = hydrophobic organic carbon).

4.2. Extended Impacts

The fate of the smoke aerosols depends greatly on the altitude of injection in the weeks and months following the pyroCb event. For the stratospheric injection, around 40% of the stratospheric aerosols are still present in the modeled atmosphere at the end of December 2017 (0.079 Tg) representing an *e*-folding time of around 5 months for these stratospheric aerosols (Figure 2a). This lifetime is in the range observed for stratospheric sulfate aerosols in medium-sized volcanic eruptions (Bluth et al., 1997). In contrast, after 3 weeks, only 7% of the initial smoke aerosol mass in the boundary layer case was present in the model resulting in an *e*-folding time of around 4 days. This lifetime is in the 5.8 ± 1.8-day range reported for BC lifetime over the northwest Pacific (Park et al., 2005). In a sensitivity test, injecting the smoke into the free troposphere (8 km) resulted in an *e*-folding lifetime of 13 days. This high sensitivity to injection altitude illustrates the documented altitude dependence of aerosol lifetime.

Throughout September of 2017, CATS observed a persistent layer of stratospheric aerosols over central Asia on many overpasses (Figures 3d–3f) that likely originated from the pyroCb event (Figure S3). At this point, GEOS-Chem had spread the pyroCb aerosols throughout the Northern Hemisphere with higher concentrations and optical depths over the Arctic as evidenced by where we find the highest radiative forcing (Figures 3a–3c; radiative forcing is discussed in section 4.3). While there is still a large mass of pyroCb aerosols present in the modeled stratosphere (Figure 2a), GEOS-Chem does not specifically place the pyroCb aerosols where the CATS overpass observed the stratospheric aerosol layer in September. Where CATS observed a persistent and somewhat defined plume, GEOS-Chem had spread the pyroCb aerosols throughout the Northern Hemisphere stratosphere. In these August and September 2017 cases, the CATS V2-01

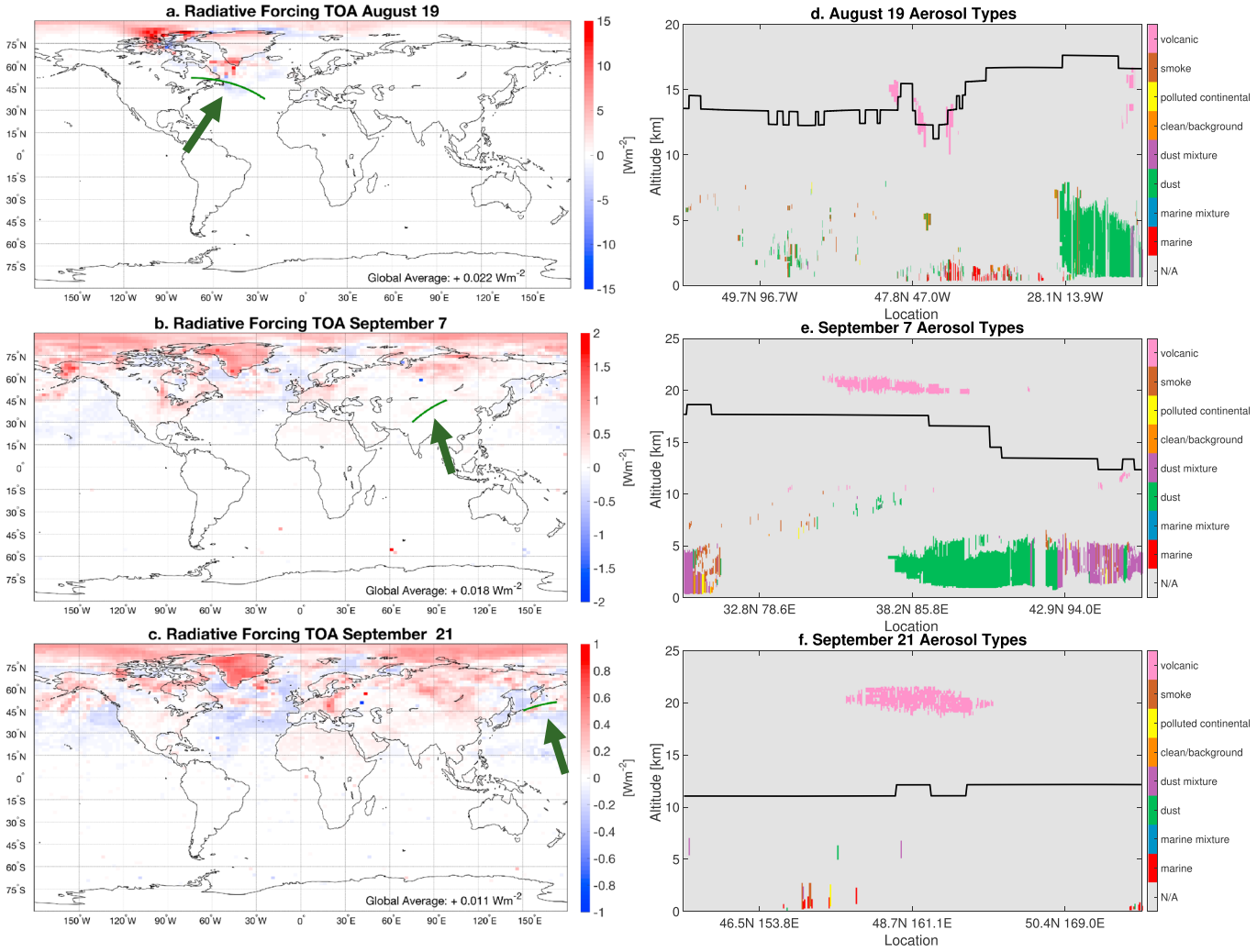

Figure 3. Top of the atmosphere (TOA) radiative forcings for 19 August (a), 7 September (b), and 21 September (c) with corresponding Cloud-Aerosol Transport System overpasses ([d]–[f], respectively). Green lines pointed out in (a)–(c) correspond to Cloud-Aerosol Transport System lidar overpasses shown in respective aerosol type subplots (d–f). Black lines in aerosol type subplots (d–f) correspond to tropopause altitudes.

aerosol typing algorithm suggests these aerosols are volcanic in origin; however, this is merely a result of the algorithm categorizing any UTLS aerosols as volcanic (Yorks et al., 2016). In the CATS V3-00 data products, which will be released shortly, this aerosol classification name has been changed to "UTLS" as a result of the observations discussed in this paper (Yorks, 2018).

4.3. Radiative Impacts

There were significant changes to the full-sky (including cloud coverage) radiative balance at the top of the atmosphere following the modeled aerosol plume when coupling the modeled results to the Fu-Liou radiative transfer model. A week after the pyroCb event when the plume was over the North Atlantic (as shown in Figure 1), we find daily averaged local changes to the shortwave radiation at the top of the atmosphere to be around 15 W/m^2 with the global average being around 0.02 W/m^2 (Figure 3a). Radiatively, the absorptive effects of the BC aerosols in the plume are stronger than the reflective effects of the OC resulting in a net warming effect on the atmosphere. This warming effect is predominantly focused over high albedo surfaces such as the Greenland Ice Sheet and the sea ice-covered Arctic Ocean. Over lower albedo areas such as the open ocean, the smoke results in slight cooling effects. These aerosols result in on average 0.7–0.9 K/day in shortwave heating in the Arctic stratosphere (north of 60°N) in the month of September (Figure 4) with the highest warming rates centered over the northernmost latitudes. The radiative forcings from the pyroCb event peak about a week after the event before decreasing over the following months as the mass of pyroCb smoke in the model subsides (Figure 2b). The net radiative forcing was between +0.02 and +0.01 W/m^2 over

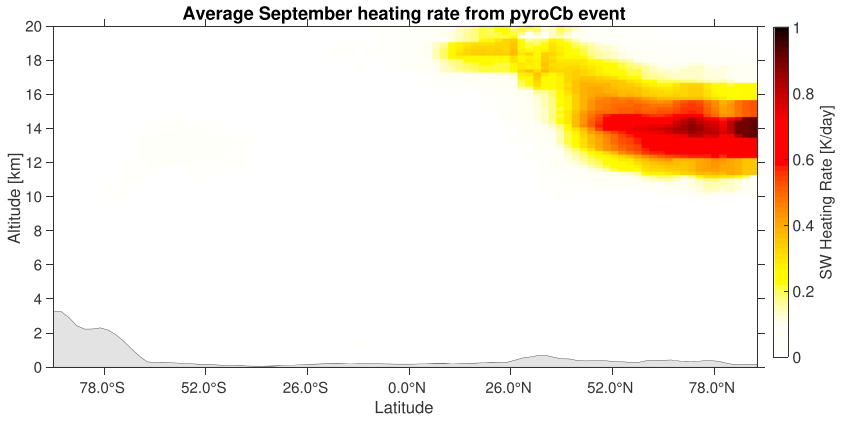

Figure 4. Zonally averaged shortwave (SW) heating rates for September 2017 (K/day) from the pyroCb aerosols.

the 2–3 months following the pyroCb event, which is substantially different from analogous volcanic studies. For example, radiative forcings from the 2008 Kasatochi eruption were between −1.3 and −0.7 W/m^2 in the 1–2 months following the eruption and −0.03 W/m^2 after 6 months (Wang et al., 2013). Yearly and global averages of eruptive volcanic radiative forcings in 2006–2012 have been found to be around −0.09 W/m^2 (Ge et al., 2016). Thus, the potential radiative impacts of multiple pyroCb events can be of a similar magnitude to volcanic events but of opposite sign. As a function of smoke AOD, the forcing in the stratospheric injection case is between 0 and +5 W/m^2 per unit AOD (550 nm) from 1 week after the event through the end of September.

Considering the opposing effects of BC and OC in the radiative transfer model, it would be expected that the radiative forcing would be sensitive to the chosen emission factors. Indeed, if the fraction of BC is increased to 12%, an emission factor typical of tropical forests (van der Werf et al., 2010), the net forcing increases significantly to around +0.15 W/m^2.

There are a few limitations and uncertainties associated with these radiative forcing calculations. We specifically note that the warming associated with the smoke aerosols is limited to the UTLS, not the lower troposphere or surface, and only takes into account the direct effects of the pyroCb smoke aerosols on the flux of outgoing shortwave radiation at the top of the atmosphere. Exploring the effects of pyroCb events in climate models would be a valuable avenue for future research as previous studies have shown that stratospheric BC can have a negative climate forcing and suppressing effect on surface temperatures once semidirect effects (effects on the thermodynamic structure of the atmosphere and tropospheric cloud coverage) and changes in longwave radiative fluxes are taken into account (Ban-Weiss et al., 2012). In addition, the forcings from the pyroCb aerosols may be greater if the aerosols are internally mixed with sulfates. This correction may increase the positive radiative forcing from BC by +50% (Kopacz et al., 2011).

5. Discussion and Conclusions

We have shown here the capacity of GEOS-Chem to model the effects of a pyroCb event. Compared to satellite measurements from CATS and CALIOP lidar and EPIC UVAI, we find GEOS-Chem accurately represents the transport of the resultant stratospheric plume of smoke aerosols when the pyroCb emissions are directly injected into the model stratosphere. When the fire emissions are emitted into the boundary layer (as is typically done in CTMs and climate models), we find GEOS-Chem fails to recreate the observed vertical aerosol distribution. This higher emission altitude has great consequences for the aerosol residence times with the stratospheric aerosols having an *e*-folding time of around 5 months and the boundary layer aerosols having an *e*-folding time of only 4 days. With modeled UTLS composition and radiative effects being sensitive to injection altitude, any attempts to include pyroCb and other biomass burning emissions in CTMs will need to strongly consider injection altitudes. Also, future 3-D biomass burning emission inventories constrained by lidar observations would equip models to better capture the broader effects resulting from pyroCb and other fires with high-altitude plumes.

Because the BC and OC components of the smoke aerosols are respectively strong absorbers and reflectors of incoming solar radiation, the net forcing is sensitive to the chosen emission factors. Using an estimate of

~6% of the smoke aerosols emitted as BC (with the remainder as OC), we find globally averaged net radiative forcings between 0 and +0.05 W/m^2 with the BC forcing being around +0.1 W/m^2 and OC around −0.1 W/m^2 in the month following the pyroCb event. This +0.1 W/m^2 BC forcing is greater than that estimated of BC's altering of ice/snowpack albedo (0.02–0.09 W/m^2; Myhre et al., 2013) and represents the effects of one large event. Future work will be needed to determine the cumulative effects of the dozens of pyroCb events that occur on a yearly basis. The net forcing is slightly positive meaning the aerosols injected into the UTLS by the pyroCb event had a net warming effect on the Earth system, especially focused in the UTLS. This is opposite the effects of volcanic events, which result in a net cooling effect on the Earth system. In addition, the carbonaceous aerosols emitted by pyroCb events would have different effects on chemical and microphysical interactions than analogous volcanic aerosols. With these different and complicated interactions, a full understanding of the responses of surface temperature and atmospheric processes to pyroCb events in future studies will require the use of global climate models. This study serves as the first attempt to provide observation-constrained insights for such climate modeling studies in terms of pyroCb smoke particle injection height, lifetime, and magnitude of UTLS heating from the pyroCb smoke aerosols.

GEOS-Chem proved well suited to quantify the effects of pyroCb events on atmospheric composition and the radiative balance of the planet provided smoke aerosols were directly injected into the stratosphere. We find the Pacific Northwest event likely resulted in a net positive radiative forcing at the top of the atmosphere. This is significantly different from analogous volcanic events and highlights the effects of the differing aerosol composition between the mostly sulfate aerosol emitting volcanic events and the carbonaceous aerosol emitting pyroCb events. Furthermore, the August 2017 fires in Washington (USA) and British Columbia (Canada) and their associated smoke plumes provide a data set to better differentiate these plumes from volcanic and other aerosols in the UTLS in space-based lidar detection algorithms (CATS and CALIOP). Considering their capacity as regular sources of persistent UTLS carbonaceous aerosols, including pyroCb events and their emissions in future studies should be considered.

Acknowledgments
This work was supported by the NASA Aura Science Team (Grant NNX17AF63G managed by Dr. Kenneth Jucks), Atmospheric Modeling and Analysis program and DSCOVR Science Team program (Grant NNX17AB05G managed by Dr. Richard Eckman), and the Office of Naval Research (ONR) Multidisciplinary University Research Initiatives (MURI) Program (under the Award N00014-16-1-2040). D. Peterson was supported by the NASA New Investigator Program (Grant NNH17ZDA001N managed by Allison Leidner). Satellite data shown in the paper can be obtained from the NASA Langley Research Center Atmospheric Science Data Center (earthdata.nasa.gov). The GEOS data used in this study/project have been provided by the Global Modeling and Assimilation Office (GMAO) at NASA Goddard Space Flight Center. The results presented in this manuscript will be made available through Coalition on Publishing Data in the Earth and Space 303 Sciences (https://copdessdirectory.osf.io). For further inquiry, please email Jun Wang (jun-wang-1@uiowa.edu) or Kenneth Christian (kenneth.e.christian@nasa.gov) for details.

References

Andreae, M. O., Rosenfeld, D., Artaxo, P., Costa, A. A., Frank, G. P., Longo, K. M., & Silva-Dias, M. a. F. (2004). Smoking rain clouds over the Amazon. *Science*, *303*, 1337–1342. http://science.sciencemag.org/content/303/5662/1337, https://doi.org/10.1126/science.1092779

Ban-Weiss, G. A., Cao, L., Bala, G., & Caldeira, K. (2012). Dependence of climate forcing and response on the altitude of black carbon aerosols. *Climate Dynamics*, *38*(5), 897–911. Retrieved from https://doi.org/10.1007/s00382-011-1052-y

Barnes, J. E., & Hofmann, D. J. (1997). Lidar measurements of stratospheric aerosol over Mauna Loa Observatory. *Geophysical Research Letters*, *24*(15), 1923–1926. Retrieved 2019-02-08, https://doi.org/10.1029/97GL01943

Bey, I., Jacob, D. J., Yantosca, R. M., Logan, J. A., Field, B. D., Fiore, A. M., & Schultz, M. G. (2001). Global modeling of tropospheric chemistry with assimilated meteorology: Model description and evaluation. *Journal of Geophysical Research*, *106*(D19), 23,073–23,095. https://doi.org/10.1029/2001JD000807

Bluth, G., Rose, W., Sprod, I., & Krueger, A. (1997). Stratospheric loading of sulfur from explosive volcanic eruptions. *The Journal of Geology*, *105*(6), 671–684. https://doi.org/10.1086/515972

Bond, T. C., Doherty, S. J., Fahey, D. W., Forster, P. M., Berntsen, T., DeAngelo, B. J., & Zender, C. S. (2013). Bounding the role of black carbon in the climate system:Ascientific assessment. *Journal of Geophysical Research: Atmospheres*, *118*, 5380–5552. https://doi.org/10.1002/jgrd.50171

Chin, M., Ginoux, P., Kinne, S., Torres, O., Holben, B. N., Duncan, B. N., & Nakajima, T. (2002). Tropospheric aerosol optical thickness from the GOCART model and comparisons with satellite and Sun photometer measurements. *Journal of the Atmospheric Sciences*, *59*(3), 461–483. https://doi.org/10.1175/1520-0469(2002)059<0461:TAOTFT>2. 0. CO;2

Clarke, A. D., Charlson, R. J., & Ogren, J. A. (1983). Stratospheric aerosol light absorption before and after El Chichon. *Geophysical Research Letters*, *10*(11), 1017–1020. https://doi.org/10.1029/GL010i011p01017

Colarco, P. R., Schoeberl, M. R., Doddridge, B. G., Marufu, L. T., Torres, O., & Welton, E. J. (2004). Transport of smoke from Canadian forest fires to the surface near Washington, D. C. :Injection height, entrainment, and optical properties. *Journal of Geophysical Research*, *109*, D06203. https://doi.org/10.1029/2003JD004248

de Laat, A. T. J., Zweers, D. C. S., Boers, R., & Tuinder, O. N. E. (2012). A solar escalator: Observationalevidence of the self-lifting of smoke and aerosols by absorption of solar radiation in the February 2009 Australian Black Saturday plume. *Journal of Geophysical Research*, *117*, D04204. https://doi.org/10.1029/2011JD017016

Field, R. D., Luo, M., Fromm, M., Voulgarakis, A., Mangeon, S., & Worden, J. (2016). Simulating the Black Saturday 2009 smoke plume with an interactive composition-climate model: Sensitivity to emissions amount, timing, and injection height. *Journal of Geophysical Research: Atmospheres*, *121*, 4296–4316. https://doi.org/10.1002/2015JD024343

Fromm, M., Alfred, J., Hoppel, K., Hornstein, J., Bevilacqua, R., Shettle, E., & Stocks, B. (2000). Observations of boreal forest fire smoke in the stratosphere by POAM III, SAGE II, and lidar in 1998. *Geophysical Research Letters*, *27*(9), 1407–1410. https://doi.org/10.1029/1999GL011200

Fromm, M., Bevilacqua, R., Servranckx, R., Rosen, J., Thayer, J. P., Herman, J., & Larko, D. (2005). Pyro-cumulonimbus injection of smoke to the stratosphere: Observations and impact of a super blowup in northwestern Canada on 34 August 1998. *Journal of Geophysical Research*, *110*, D08205. https://doi.org/10.1029/2004JD005350

Fromm, M., Lindsey, D. T., Servranckx, R., Yue, G., Trickl, T., Sica, R., & Godin-Beekmann, S. (2010). The untold story of pyro cumulonimbus. *Bulletin of the American Meteorological Society*, *91*(9), 1193–1210. https://doi.org/10.1175/2010BAMS3004.1

Fu, Q., & Liou, K. N. (1992). On the correlated k-distribution method for radiative transfer in nonhomogeneous atmospheres. *Journal of the Atmospheric Sciences*, *49*(22), 2139–2156. https://doi.org/10.1175/1520-0469(1992)049<2139:OTCDMF>2.0.CO;2

Fu, Q., & Liou, K. N. (1993). Parameterization of the radiative properties of cirrus clouds. *Journal of the Atmospheric Sciences*, *50*(13), 2008–2025. https://doi.org/10.1175/1520-0469(1993)050<2008:POTRPO>2.0.CO;2

Ge, C., Wang, J., Carn, S., Yang, K., Ginoux, P., & Krotkov, N. (2016). Satellite-based global volcanic SO_2 emissions and sulfate direct radiative forcing during 2005–2012. *Journal of Geophysical Research: Atmospheres*, *121*, 3446–3464. https://doi.org/10.1002/2015JD023134

Gu, Y., Liou, K. N., Xue, Y., Mechoso, C. R., Li, W., & Luo, Y. (2006). Climatic effects of different aerosol types in china simulated by the ucla general circulation model. *Journal of Geophysical Research*, *111*, D15201. https://doi.org/10.1029/2005JD006312

Herman, J. R., Bhartia, P. K., Torres, O., Hsu, C., Seftor, C., & Celarier, E. (1997). Global distribution of UV-absorbing aerosols from Nimbus 7/TOMS data. *Journal of Geophysical Research*, *102*(D14), 16,911–16,922. https://doi.org/10.1029/96JD03680

Hughes, E. J., Yorks, J. E., Krotov, N. A., da Silva, A. M., & McGill, M. J. (2016). Using CATS near-real-time lidar observations to monitor and constrain volcanic sulfur dioxide (SO2) forecasts. *Geophysical Research Letters*, *43*, 11,089–11,097. https://doi.org/10.1002/2016GL070119

Jacobson, M. Z. (2001). Strong radiative heating due to the mixing state of black carbon in atmospheric aerosols. *Nature*, *409*, 695–697. https://doi.org/10.1038/35055518

Keller, C. A., Long, M. S., Yantosca, R. M., Da Silva, A. M., Pawson, S., & Jacob, D. J. (2014). HEMCO v1. 0: A versatile, ESMF-compliant component for calculating emissions in atmospheric models. *Geoscientific Model Development*, *7*(4), 1409–1417. https://doi.org/https://doi.org/10.5194/gmd-7-1409-2014

Khaykin, S. M., GodinBeekmann, S., Hauchecorne, A., Pelon, J., Ravetta, F., & Keckhut, P. (2018). Stratospheric smoke with unprecedentedly high backscatter observed by lidars above southern France. *Geophysical Research Letters*, *45*, 1639–1646. https://doi.org/10.1002/2017GL076763

Koch, D., Schulz, M., Kinne, S., McNaughton, C., Spackman, J. R., Balkanski, Y., & Zhao, Y. (2009). Evaluation of black carbon estimations in global aerosol models. *Atmospheric Chemistry and Physics*, *9*(22), 9001–9026. https://doi.org/10.\ignorespaces5194/acp-9-9001-2009

Kopacz, M., Mauzerall, D. L., Wang, J., Leibensperger, E. M., Henze, D. K., & Singh, K. (2011). Origin and radiative forcing of black carbon transported to the Himalayas and Tibetan Plateau. *Atmospheric Chemistry and Physics*, *11*(6), 2837–2852. https://doi.org/10.5194/acp-11-2837-2011

Kremser, S., Thomason, L. W., Hobe, M. V., Hermann, M., Deshler, T., Timmreck, C., & Meland, B. (2016). Stratospheric aerosol observations, processes, and impact on climate. *Reviews of Geophysics*, *54*, 278–335. https://doi.org/10.1002/2015RG000511

Leung, F. Y. T., Logan, J. A., Park, R., Hyer, E., Kasischke, E., Streets, D., & Yurganov, L. (2007). Impacts of enhanced biomass burning in the boreal forests in 1998 on tropospheric chemistry and the sensitivity of model results to the injection height of emissions. *Journal of Geophysical Research*, *112*, D10313. https://doi.org/10.1029/2006JD008132

Lucchesi, R. (2017). File specification for GEOS-5 FP.GMAO office note no.4 (version 1. 1) (*Tech. Rep.*): GMAO. https://gmao.gsfc.nasa.gov/products/documents/GEOS_5_FP_File_Specification_ON4v1_1.pdf

Marshak, A., Herman, J., Adam, S., Karin, B., Carn, S., Cede, A., & Yang, Y. (2018). Earth observations from DSCOVR EPIC instrument. *Bulletin of the American Meteorological Society*, *99*(9), 1829–1850. https://doi.org/10.1175/BAMS-D-17-0223.1

McGill, M. J., Yorks, J. E., Scott, V. S., Kupchock, A. W., & Selmer, P. A. (2015). The Cloud-Aerosol Transport System (CATS): A technology demonstration on the International Space Station. In *Lidar Remote Sensing for Environmental Monitoring XV* . San Diego, CA: SPIE. https://doi.org/10.1117/12.2190841

Myhre, G., Shindell, F. M., Breon, W., Collins, J., Fuglestvedt, J., Huang, J., & Zhang, H. (2013). Anthropogenic and natural radiative forcings, *Climate Change 2013: The Physical Science Basis. Contribution of Working Group I to the Fifth Assessment Report of the Intergovernmental Panel on Climate Change* (pp. 659–740). Cambridge,United Kingdom: Cambridge University Press.

Park, R. J., Jacob, D. J., Chin, M., & Martin, R. V. (2003). Sources of carbonaceous aerosols over the United States and implications for natural visibility. *Journal of Geophysical Research*, *108*(D12), 4355. https://doi.org/10.1029/2002JD003190

Park, R. J., Jacob, D. J., Palmer, P. I., Clarke, A. D., Weber, R. J., Zondlo, M. A., & Bond, T. C. (2005). Export efficiency of black carbon aerosol in continental outflow: Global implications. *Journal of Geophysical Research*, *110*, D11205. https://doi.org/10.1029/2004JD005432

Paugam, R., Wooster, M., Freitas, S., & Val Martin, M. (2016). A review of approaches to estimate wildfire plume injection height within large-scale atmospheric chemical transport models. *Atmospheric Chemistry and Physics*, *16*(2), 907–925. https://doi.org/10.\ignorespaces5194/acp-16-907-2016

Peterson, D. A., Campbell, J. R., Hyer, E. J., Fromm, M. D., Kablick, G. P., Cossuth, J. H., & DeLand, M. T. (2018). Wildfire-driven thunderstorms cause a volcano-like stratospheric injection of smoke. *npj Climate and Atmospheric Science*, *1*(1), 30. https://doi.org/10.1038/s41612-018-0039-3

Peterson, D. A., Fromm, M. D., Solbrig, J. E., Hyer, E. J., Surratt, M. L., & Campbell, J. R. (2016). Detection and inventory of intense pyroconvection in western North America using GOES-15 daytime infrared data. *Journal of Applied Meteorology and Climatology*, *56*(2), 471–493. https://doi.org/10.\ignorespaces1175/JAMC-D-16-0226.1

Peterson, D. A., Hyer, E. J., Campbell, J. R., Fromm, M. D., Hair, J. W., Butler, C. F., & Fenn, M. A. (2014). The 2013 Rim Fire: Implications for predicting extreme fire spread, pyroconvection, and smoke emissions. *Bulletin of the American Meteorological Society*, *96*(2), 229–247. https://doi.org/10.1175/BAMS-D-14-00060.1

Peterson, D. A., Hyer, E. J., Campbell, J. R., Solbrig, J. E., & Fromm, M. D. (2016). A conceptual model for development of intense pyrocumulonimbus in western North America. *Monthly Weather Review*, *145*(6), 2235–2255. https://doi.org/10.1175/MWR-D-16-0232.1

Ramanathan, V., & Carmichael, G. (2008). Global and regional climate changes due to black carbon. *Nature Geoscience*, *1*(4), 221–227. https://doi.org/10.1038/ngeo156

Robock, A. (2000). Volcanic eruptions and climate. *Reviews of Geophysics*, *38*(2), 191–219. https://doi.org/10.1029/1998RG000054

Schwarz, J. P., Spackman, J. R., Fahey, D. W., Gao, R. S., Lohmann, U., Stier, P., & Reeves, J. M. (2008). Coatings and their enhancement of black carbon light absorption in the tropical atmosphere. *Journal of Geophysical Research*, *113*, D03203. https://doi.org/10.1029/2007JD009042

Siddaway, J. M., & Petelina, S. V. (2011). Transport and evolution of the 2009 Australian Black Saturday bushfire smoke in the lower stratosphere observed by OSIRIS on Odin. *Journal of Geophysical Research*, *116*, D06203. https://doi.org/10.1029/2010JD015162

Torres, O., Bhartia, P. K., Herman, J. R., Ahmad, Z., & Gleason, J. (1998). Derivation of aerosol properties from satellite measurements of backscattered ultraviolet radiation: Theoretical basis. *Journal of Geophysical Research*, *103*(D14), 17,099–17,110. https://doi.org/310.1029/98JD00900

Turco, R. P., Whitten, R. C., & Toon, O. B. (1982). Stratospheric aerosols: Observation and theory. *Reviews of Geophysics*, *20*(2), 233–279. https://doi.org/10.1029/RG020i002p00233

Turquety, S., Logan, J. A., Jacob, D. J., Hudman, R. C., Leung, F. Y., Heald, C. L., & Sachse, G. W. (2007). Inventory of boreal fire emissions for North America in 2004: Importance of peat burning and pyroconvective injection. *Journal of Geophysical Research*, *112*(D12S03). https://doi.org/10.1029/2006JD007281

Val Martin, M., Logan, J. A., Kahn, R. A., Leung, F. Y., Nelson, D. L., & Diner, D. J. (2010). Smoke injection heights from fires in North America: Analysis of 5 years of satellite observations. *Atmospheric Chemistry and Physics*, *10*(4), 1491–1510. https://doi.org/10.5194/acp-10-1491-2010

van der Werf, G. R., Randerson, J. T., Giglio, L., Collatz, G. J., Mu, M., Kasibhatla, P. S., & Leeuwen, T. T. v. (2010). Global fire emissions and the contribution of deforestation,savanna, forest,agricultural,and peat fires (1997–2009). *Atmospheric Chemistry and Physics*, *10*(23), 11,707–11,735. https://doi.org/10.5194/acp-10-11707-2010

Wang, J., & Christopher, S. A. (2006). Mesoscale modeling of central American smoke transport to the united states: 2. Smoke radiative impact on regional surface energy budget and boundary layer evolution. *Journal of Geophysical Research*, *111*, D14S92. https://doi.org/10.1029/2005JD006720

Wang, J., Christopher, S. A., Nair, U. S., Reid, J. S., Prins, E. M., Szykman, J., & Hand, J. L. (2006). Mesoscale modeling of Central American smoke transport to the United States: 1. Top-down assessment of emission strength and diurnal variation impacts. *Journal of Geophysical Research*, *111*, D05S17. https://doi.org/10.1029/2005JD006416

Wang, J., Jacob, D. J., & Martin, S. T. (2008). Sensitivity of sulfate direct climate forcing to the hysteresis of particle phase transitions. *Journal of Geophysical Research*, *113*, D11207. https://doi.org/10.1029/2007JD009368

Wang, J., Park, S., Zeng, J., Ge, C., Yang, K., Carn, S., & Omar, A. H. (2013). Modeling of 2008 Kasatochi volcanic sulfate direct radiative forcing: assimilation of OMI SO_2 plume height data and comparison with MODIS and CALIOP observations. *Atmospheric Chemistry and Physics*, *13*(4), 1895–1912. https://doi.org/10.5194/acp-13-1895-2013

Wiedinmyer, C., Akagi, S. K., Yokelson, R. J., Emmons, L. K., Al-Saadi, J. A., Orlando, J. J., & Soja, A. J. (2011). The Fire INventory from NCAR (FINN): A high resolution global model to estimate the emissions from open burning. *Geoscientific Model Development*, *4*(3), 625–641. https://doi.org/10.5194/gmd-4-625-2011

Winker, D. M., Vaughan, M. A., Omar, A., Hu, Y., Powell, K. A., Liu, Z., & Young, S. A. (2009). Overview of the CALIPSO mission and CALIOP data processing algorithms. *Journal of Atmospheric and Oceanic Technology*, *26*(11), 2310–2323. https://doi.org/10.1175/2009JTECHA1281.1

Woods, D. C., & Chuan, R. L. (1983). Size-specific composition of aerosols in the El Chichon volcanic cloud. *Geophysical Research Letters*, *10*(11), 1041–1044. https://doi.org/10.1029/GL010i011p01041

Xu, X., Wang, J., Wang, Y., Zeng, J., Torres, O., Yang, Y., & Miller, S. (2017). Passive remote sensing of altitude and optical depth of dust plumes using the oxygen A and B bands: First results from EPIC/DSCOVR at Lagrange-1 point. *Geophysical Research Letters*, *44*, 7544–7554. https://doi.org/10.1002/2017GL073939

Yorks, J. E. (2018). CATS data release notes: L1B Version 3. 00,L2O Version 3. 00,Cats data release notes: L1b version 3. 00,l2o version 3. 00. NASA Goddard Space Flight Center, https://cats.gsfc.nasa.gov/media/docs/CATS_Release_Notes7.pdf

Yorks, J. E., McGill, M. J., Palm, S. P., Hlavka, D. L., Selmer, P. A., Nowottnick, E. P., & Hart, W. D. (2016). An overview of the CATS level 1 processing algorithms and data products. *Geophysical Research Letters*, *43*, 4632–4639. https://doi.org/10.1002/2016GL068006